Textures of Regional Metamorphism

- Dynamothermal (crystallization under dynamic conditions)
- Orogeny - long-term mountain-building
  - May comprise several Tectonic Events
    - May have several Deformational Phases
- May have an accompanying Metamorphic Cycles with one or more Reaction Events

Progressive syntectonic metamorphism of a volcanic graywacke, New Zealand. From Best (1982). *Igneous and Metamorphic Petrology*. W. H. Freeman. San Francisco.

Progressive syntectonic metamorphism of a volcanic graywacke, New Zealand. From Best (1982). *Igneous and Metamorphic Petrology* W. H. Freeman. San Francisco.

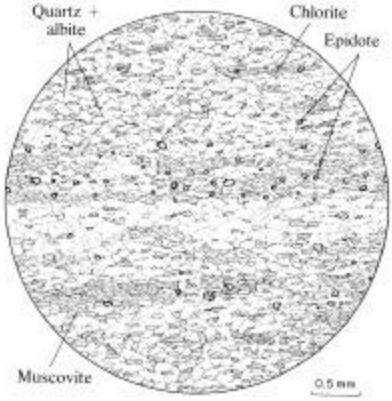

Progressive syntectonic metamorphism of a volcanic graywacke, New Zealand. From Best (1982). *Igneous and Metamorphic Petrology* W. H. Freeman. San Francisco.

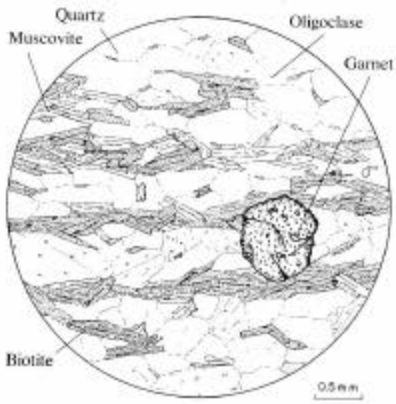

Progressive syntectonic metamorphism of a volcanic graywacke, New Zealand. From Best (1982). *Igneous and Metamorphic Petrology* W. H. Freeman. San Francisco.

Fig 23-21 Types of foliations

a. Compositional layering

b. Preferred orientation of platy minerals

c. Shape of deformed grains

d. Grain size variation

e. Preferred orientation of platy minerals in a matrix without preferred orientation

f. Preferred orientation of lenticular mineral aggregates

g. Preferred orientation of fractures

h. Combinations of the above

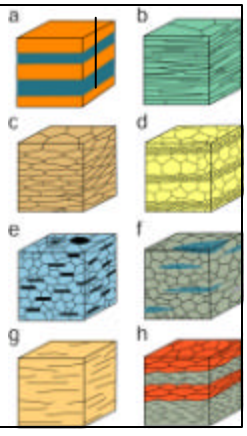

Figure 23-21. Types of fabric elements that may define a foliation. From Turner and Weiss (1963) and Passchier and Trouw (1996).

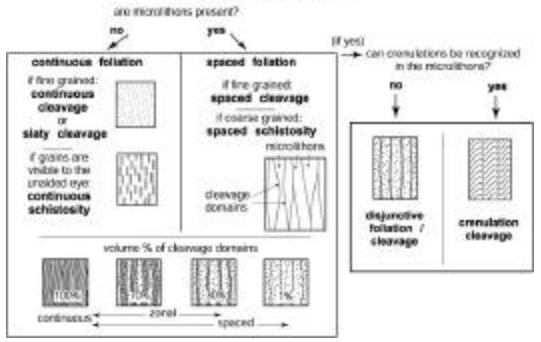

Figure 23-22. A morphological (non-genetic) classification of foliations. After Powell (1979) *Tectonophys.*, 58, 21-34; Borradaile *et al* (1982) *Atlas of Deformational and Metamorphic Rock Fabrics*. Springer- Verlag; and Passchier and Trouw (1996) *Microtectonics*. Springer- Verlag.

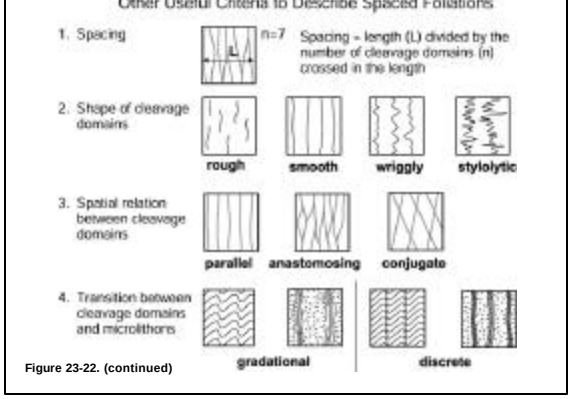

Figure 23-22. (continued)

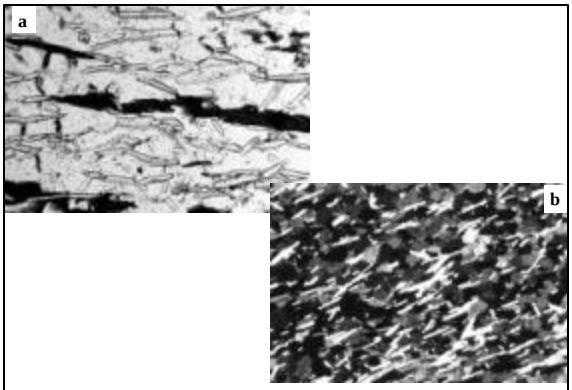

Figure 23-23. Continuous schistosity developed by dynamic recrystallization of biotite, muscovite, and quartz. a. Plane-polarized light, width of field 1 mm. b. Crossed-polars, width of field 2 mm. Although there is a definite foliation in both samples, the minerals are entirely strain-free.

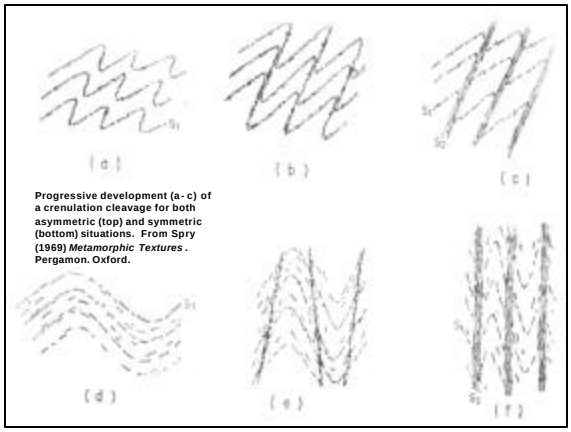

Progressive development (a- c) of a crenulation cleavage for both asymmetric (top) and symmetric (bottom) situations. From Spry (1969) *Metamorphic Textures*. Pergamon. Oxford.

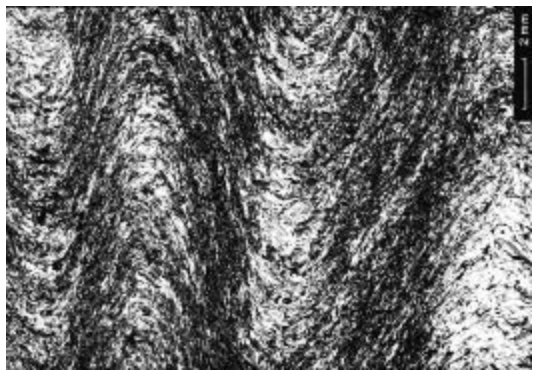

Figure 23-24a. Symmetrical crenulation cleavages in amphibole - quartz-rich schist. Note concentration of quartz in hinge areas. From Borradaile *et al*. (1982) *Atlas of Deformational and Metamorphic Rock Fabrics*. Springer-Verlag.

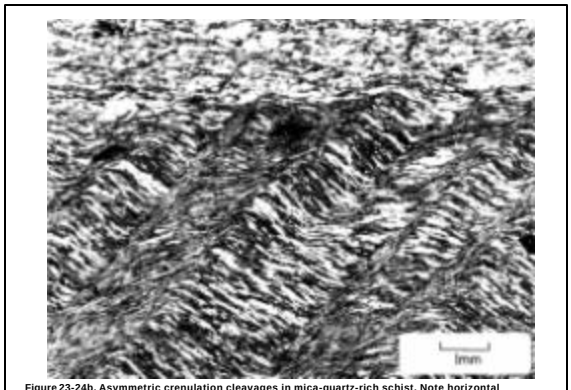

Figure 23-24b. Asymmetric crenulation cleavages in mica-quartz-rich schist. Note horizontal compositional layering (relict bedding) and preferential dissolution of quartz from one limb of the folds. From Borradaile *et al*. (1982) *Atlas of Deformational and Metamorphic Rock Fabrics*. Springer-Verlag.

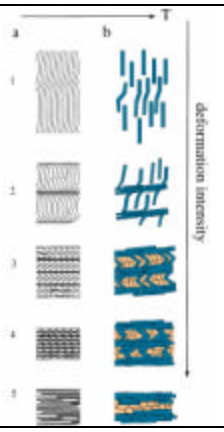

Figure 23-25. Stages in the development of crenulation cleavage as a function of temperature and intensity of the second deformation. From Passchier and Trouw (1996) *Microtectonics*. Springer-Verlag.

Development of S_2 micas depends upon T and the intensity of the second deformation

Types of lineations

a. Preferred orientation of elongated mineral aggregates

b. Preferred orientation of elongate minerals

c. Lineation defined by platy minerals

d. Fold axes (especially of crenulations)

e. Intersecting planar elements.

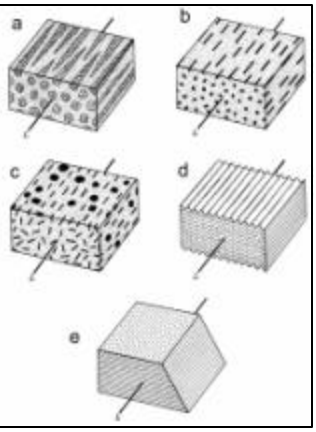

Figure 23-26. Types of fabric elements that define a lineation. From Turner and Weiss (1963) *Structural Analysis of Metamorphic Tectonites*. McGraw Hill.

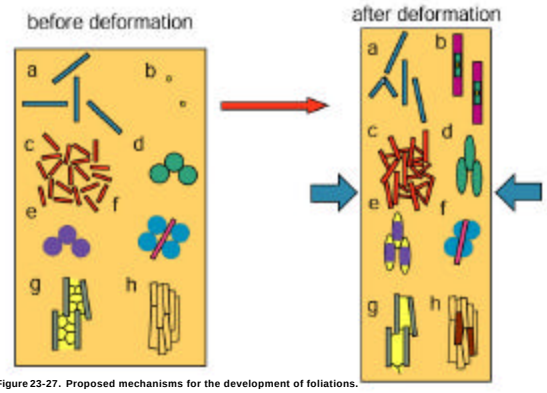

Figure 23-27. Proposed mechanisms for the development of foliations. After Passchier and Trouw (1996) Microtectonics. Springer- Verlag.

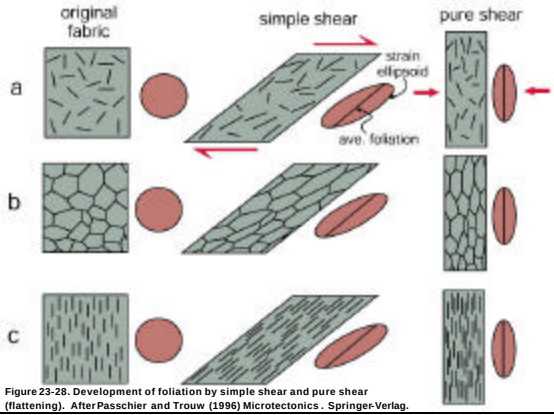

Figure 23-28. Development of foliation by simple shear and pure shear (flattening). After Passchier and Trouw (1996) Microtectonics. Springer-Verlag.

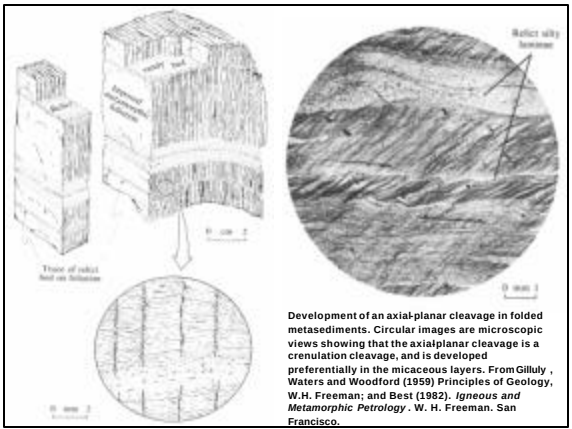

Development of an axial-planar cleavage in folded metasediments. Circular images are microscopic views showing that the axial-planar cleavage is a crenulation cleavage, and is developed preferentially in the micaceous layers. From Gilluly, Waters and Woodford (1959) Principles of Geology, W.H. Freeman; and Best (1982). *Igneous and Metamorphic Petrology*. W. H. Freeman. San Francisco.

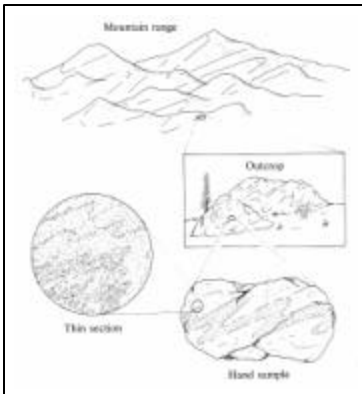

Diagram showing that structural and fabric elements are generally consistent in style and orientation at all scales. From Best (1982). *Igneous and Metamorphic Petrology*. W. H. Freeman. San Francisco.

Pre-kinematic crystals

a. Bent crystal with undulose extinction
b. Foliation wrapped around a porphyroblast
c. Pressure shadow or fringe
d. Kink bands or folds
e. Microboudinage
f. Deformation twins

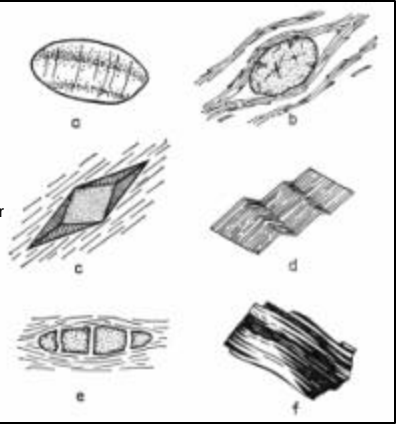

Figure 23-34. Typical textures of pre-kinematic crystals. From Spry (1969) *Metamorphic Textures*. Pergamon. Oxford.

Post-kinematic crystals

a. Helicitic folds **b.** Randomly oriented crystals **c.** Polygonal arcs **d.** Chiastolite **e.** Late, inclusion-free rim on a poikiloblast (?) **f.** Random aggregate pseudomorph

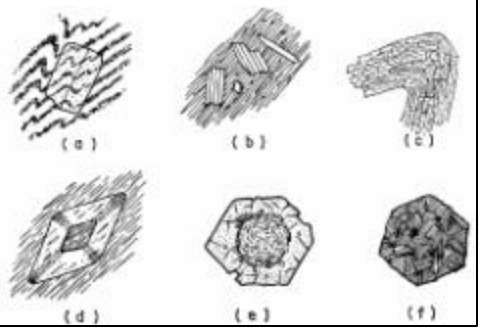

Figure 23-35. Typical textures of post-kinematic crystals. From Spry (1969) *Metamorphic Textures*. Pergamon. Oxford.

Syn-kinematic crystals

Paracrystalline microboudinage

Spiral Porphyroblast

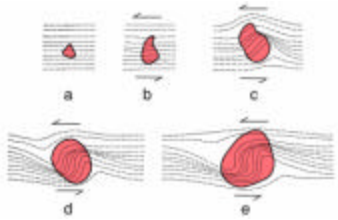

Figure 23-38. Traditional interpretation of spiral S_i train in which a porphyroblast is rotated by shear as it grows. From Spry (1969) *Metamorphic Textures*. Pergamon. Oxford.

Figure 23-36. Syn-crystallization micro-boudinage. Syn-kinematic crystal growth can be demonstrated by the color zoning that grows and progressively fills the gap between the separating fragments. After Misch (1969) *Amer. J. Sci.*, 267, 43-63.

Syn-kinematic crystals

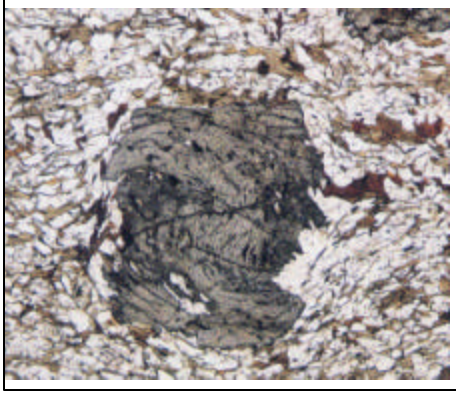

Figure 23-38. Spiral S_i train in garnet, Connemara, Ireland. Magnification ~20X. From Yardley *et al* (1990) *Atlas of Metamorphic Rocks and their Textures*. Longmans.

Syn-kinematic crystals

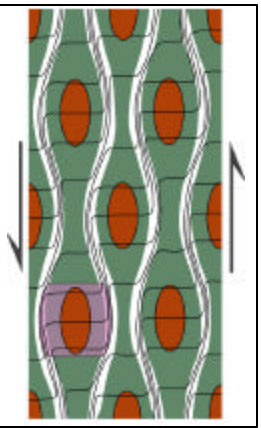

Figure 23-40. Non-uniform distribution of shear strain as proposed by Bell *et al*. (1986) *J. Metam. Geol.*, 4, 37-67. Blank areas represent high shear strain and colored areas are low-strain. Lines represent initially horizontal inert markers (S_i). Note example of porphyroblast growing preferentially in low-strain regions.

Syn-kinematic crystals

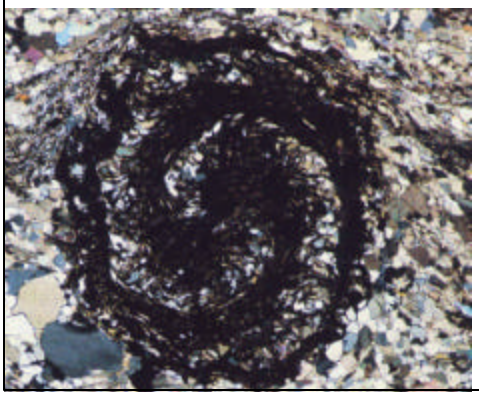

Figure 23-38. "Snowball garnet" with highly rotated spiral S_i. Porphyroblast is ~ 5 mm in diameter. From Yardley *et al* (1990) *Atlas of Metamorphic Rocks and their Textures*. Longmans.

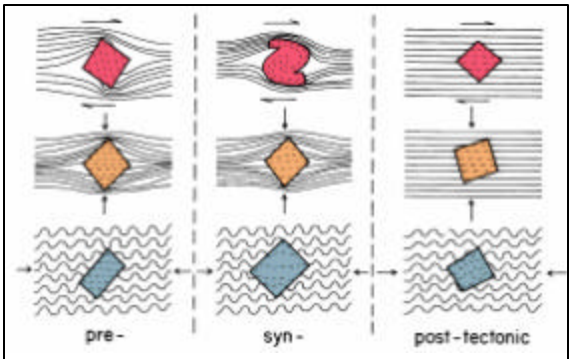

Figure 23-37. S_i characteristics of clearly pre-, syn-, and post-kinematic crystals as proposed by Zwart (1962). a. Progressively flattened S_i from core to rim. b. Progressively more intense folding of S_i from core to rim. c. Spiraled S_i due to rotation of the matrix or the porphyroblast during growth. After Zwart (1962) *Geol. Rundschau*, 52, 38-65.

Analysis of Deformed Rocks

- Deformational events: D_1 D_2 D_3 …
- Metamorphic events: M_1 M_2 M_3 …
- Foliations: S_o S_1 S_2 S_3 …
- Lineations: L_o L_1 L_2 L_3 …
- Plot on a metamorphism-deformation-time plot showing the crystallization of each mineral

Analysis of Deformed Rocks

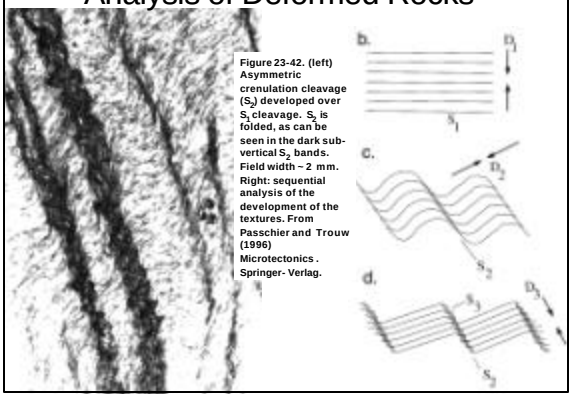

Figure 23-42. (left) Asymmetric crenulation cleavage (S_2) developed over S_1 cleavage. S_1 is folded, as can be seen in the dark sub-vertical S_2 bands. Field width ~ 2 mm. Right: sequential analysis of the development of the textures. From Passchier and Trouw (1996) Microtectonics. Springer- Verlag.

Analysis of Deformed Rocks

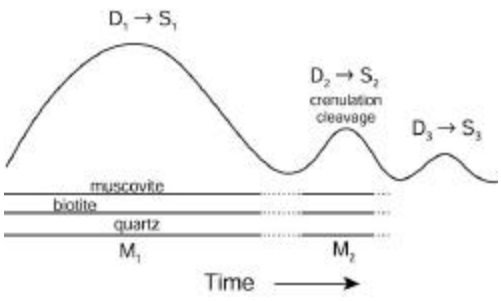

Figure 23-43. Graphical analysis of the relationships between deformation (D), metamorphism (M), mineral growth, and textures in the rock illustrated in Figure 2 3-42. Winter (2001) *An Introduction to Igneous and Metamorphic Petrology*. Prentice Hall.

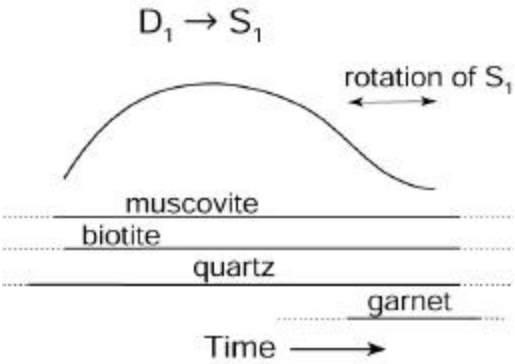

Figure 23-45. Graphical analysis of the relationships between deformation (D), metamorphism (M), mineral growth, and textures in the rock illustrated in Figure 23-44. Winter (2001) *An Introduction to Igneous and Metamorphic Petrology*. Prentice Hall.

Figure 23-46. Textures in a hypothetical andalusite porphyroblast-mica schist. After Bard (1986) *Microtextures of Igneous and Metamorphic Rocks*. Reidel. Dordrecht.

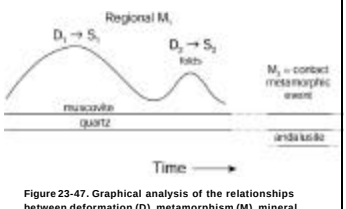

Figure 23-47. Graphical analysis of the relationships between deformation (D), metamorphism (M), mineral growth, and textures in the rock illustrated in Figure 23-46. Winter (2001) *An Introduction to Igneous and Metamorphic Petrology*. Prentice Hall.

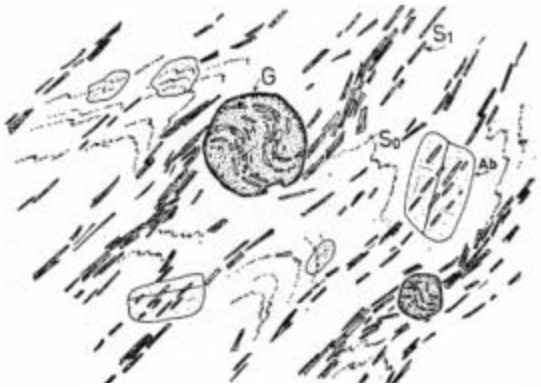

Figure 23-48a. Interpreted sequential development of a polymetamorphic rock. From Spry (1969) *Metamorphic Textures*. Pergamon. Oxford.

Figure 23-48b. Interpreted sequential development of a polymetamorphic rock. From Spry (1969) *Metamorphic Textures* . Pergamon. Oxford.

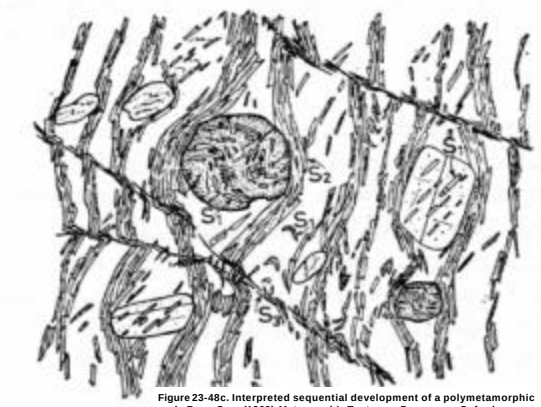

Figure 23-48c. Interpreted sequential development of a polymetamorphic rock. From Spry (1969) *Metamorphic Textures* . Pergamon. Oxford.

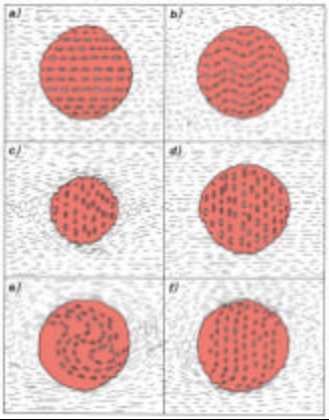

Post-kinematic: S_i is identical to and continuous with S_e

Pre-kinematic: Porphyroblasts are post-S_2. S_i is inherited from an earlier deformation. S_e is compressed about the porphyroblast in (c) and a pressure shadow develops.

Syn-kinematic: Rotational porphyroblasts in which S_i is continuous with S_e suggesting that deformation did not outlast porphyroblast growth.

From Yardley (1989) An Introduction to Metamorphic Petrology. Longman.

Deformation may not be of the same style or even coeval throughout an orogen

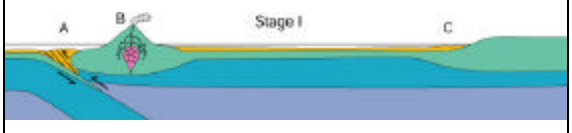

Stage I: D_1 in forearc (A) migrates away from the arc over time. Area (B) may have some deformation associated with pluton emplacement, area (C) has no deformation at all

Figure 23-49. Hypothetical development of an orogenic belt involving development and eventual accretion of a volcanic island arc terrane. After Passchier and Trouw(1996) Microtectonics. Springer-Verlag.

Deformation may not be of the same style or even coeval throughout an orogen

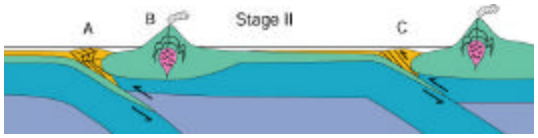

Stage II: D_2 overprints D_1 in forearc (A) in the form of sub-horizontal folding and back-thrusting as pushed against arc crust. Area (C) begins new subduction zone with thrusting and folding migrating toward trench.

Figure 23-49. Hypothetical development of an orogenic belt involving development and eventual accretion of a volcanic island arc terrane. After Passchier and Trouw(1996) Microtectonics. Springer-Verlag.

Deformation may not be of the same style or even coeval throughout an orogen

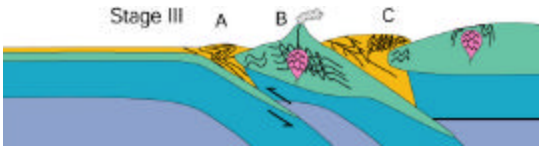

Stage III: Accretion deforms whole package. More resistant arc crust gets a D_1 event. D_2 overprints D_1 in forearc (A) and in pluton-emplacement structures in (B). Area (C) in the suture zone gets D_3 overprinting D_2 recumbent folds on D_1 foliations.

Figure 23-49. Hypothetical development of an orogenic belt involving developme nt and eventual accretion of a volcanic island arc terrane. After Passchier and Trouw (1996) Microtectonics. Springer-Verlag.

Deformation may not be of the same style or even coeval throughout an orogen

The orogen as it may now appear following uplift and erosion.

Figure 23-49. Hypothetical development of an orogenic belt involving development and eventual accretion of a volcanic island arc terrane. After Passchier and Trouw (1996) Microtectonics. Springer-Verlag.

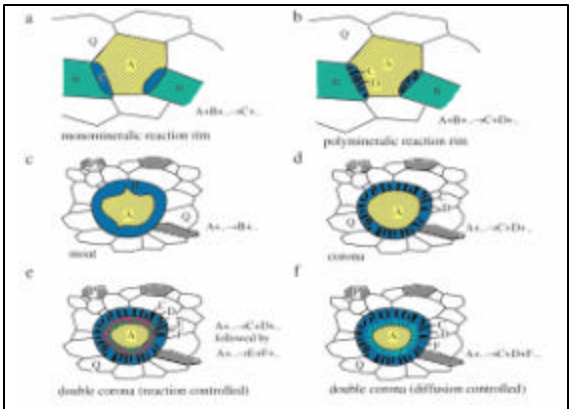

Figure 23-53. Reaction rims and coronas. From Passchierand Trouw(1996) Microtectonics . Springer-Verlag.

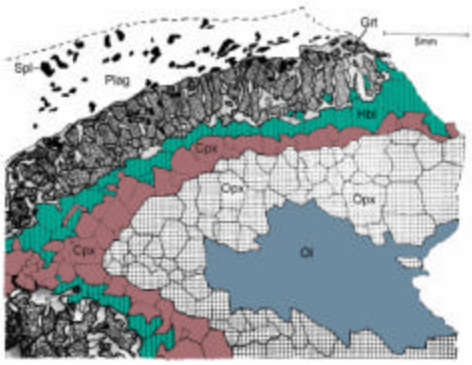

Figure 23-54. Portion of a multiplecoronite developed as concentric rims due to reaction at what was initially the contact between an olivine megacryst and surroundi ng plagioclase in anorthosites of the upper Jotun Nappe, W. Norway. From Griffen (1971) *J. Petrol.*, 12, 219-243.

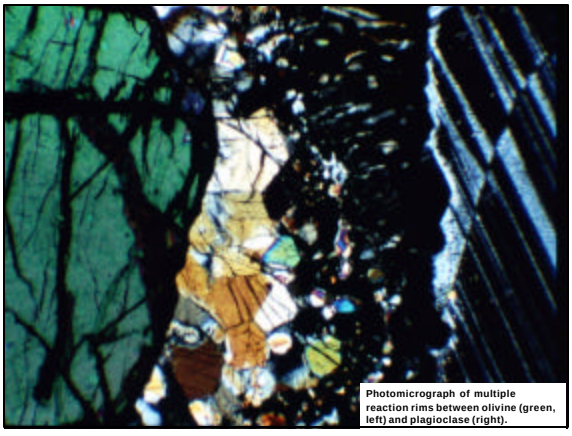

Photomicrograph of multiple reaction rims between olivine (green, left) and plagioclase (right).

Coronites in outcrop. Cores of orthopyroxene (brown) with successive rims of clinopyroxene (dark green) and garnet (red) in an anorthositic matrix. Austrheim, Norway.